

Topological Data Analysis for Image Forgery Detection

Ahmed K. Al-Jaberi¹, Aras Asaad², Sabah A. Jassim³, Naseer Al-Jawad⁴,

¹Senior Lecturer, Mathematics department, college of education for pure science, the University of Basrah,

²Lecturer, ³Prof and Head, ⁴Senior Lecturer, School of Computing, the University of Buckingham, UK.

Abstract

The manipulation of digital images has become easy due to powerful computers, advanced photo-editing software packages and high-resolution image-capturing devices. The identification of image authenticity has received much attention because of the increasing power of image editing methods. Object removal is an image forgery technique, which is usually achieved by the Exemplar-Based Inpainting (EBI) method without any noticeable traces. Some legal issues may arise when a tampered image cannot be distinguished from a real one by visual examination. Therefore the manipulation of digital images has become a huge challenge to passive image forensics. There are a lot of forgery techniques that use to detect on these images after removing the object, but these techniques have limitations when used some post-processing operations such as super-resolution processing, noise addition, blurring and compression processes. To address this issue, this paper proposes a novel forgery detection technique to recognize tampered inpainting images, using topological data analysis (TDA) approach. TDA is a mathematical approach concern studying shapes or objects to gain information about connectivity and closeness property of those objects. This proposed technique is applied for a large number of natural images with getting a good results.

Keywords: Image forgery. Image inpainting. Topological Data Analysis. Local Binary patterns. *k*NN classifier.

Introduction

In recent years, the field of digital image forgery detection has remained active and has received significant interest from the scientific community. A wide-ranging study about image forgery detection have been introduced in ⁽¹⁾.

A copy-move and object removal are a famous forgeries processes at this time. There are a lot of techniques for detecting the copy-move regions in images in the literature, also there are a lot of techniques for detecting the forgery regions in images. However, we will focus on techniques for the detection of object removals in an image, which is usually completed by EBI method in an unnoticeable way. Up to now, there are few works which report about the blind detection of image inpainting ^{(2), (3), (4), (5), (6)}.

As the first attempt, the authors in ⁽²⁾ introduced a forgery detection method for EBI based on zero-connectivity features, and fuzzy membership is proposed to detect specific image doctoring to yield the degree of matching of blocks in suspicious regions and identified forged regions by the fuzzy membership. However, this method failed to detect the forged regions in the compressed and JPEG images.

Later, the authors in ⁽³⁾ presented an automatic forgery detection method for EBI process. The proposed method contains two major processes: suspicious region detection and forged region identification. The proposed method performs well with regard to both accuracy and speed while detecting forged regions. However, this method still incapable to locate the forged regions of small sizes.

Therefore, Bacchuwar et al. in ⁽⁴⁾ proposed a novel method to detect inpainting forgery and copy-move regions using a jump patch-block matching, which makes this method robust and faster than the already existing methods. This method reduces computational costs.

Corresponding author:

Ahmed K. Al-Jaberi .

E-mail: ahmed.shanan@uobasrah.edu.iq

In recent work, the authors in ⁽⁵⁾ presented an efficient forgery detection technique for object removal by EBI method. This proposed technique combines central pixel mapping, greatest zero-connectivity component labelling and fragment splicing detection. The proposed technique has succeeded in detecting the tampered regions in images and reduction of computational complexity; but this method fail to when those inpainted images are further subjected to some post-processing operations such as super-resolution process, noise addition, blurring, and compression.

Therefore, the authors in ⁽⁶⁾ proposed a hybrid forensic technique to detect object removal in the images. First, the technique in ⁽⁵⁾ is used to detect whether the image is forged or not. Second, the DCT is computed for the undetectable images, then the joint probability density matrix is computed for each difference array to model the correlations among adjacent DCT coefficients. This technique has succeeded in detecting the object removal either with or without post-processing but this work still has some limitations, because it is only working if a candidate image is forged. So to detect the forged image either with or without post-processing, we propose a new technique based on the TDA approach.

The rest of the paper organized as follows. The topological data (image) analysis is clarified. After that Local binary patterns are introduced as an image texture descriptor to build Rips complexes. Then TDA approach is proposed to detect which of these images has had an object removed from it. Next the experimental results of the proposed technique are illustrated. Finally, conclusion and future work will be presented.

Topological Data/Image Analysis

The topology has used to study the shapes of data (objects) ^{(7), (8), (9)}. Once the shape of the data (e.g. images) constructed, then topology has rich tools to study the connectivity and closeness properties of that shape/object, using a finite combinatorial process known as Simplicial Complex (SC). Roughly speaking simplicial complexes are made up of zero-dimensional simplices (i.e. vertices), then building one-dimensional simplices (i.e. edges between the vertices) from them, then 2nd dimensional simplices (i.e. triangles) from zero and one-dimensional simplices and then higher dimensional simplices are constructed similarly. Finally, one gets a

SC by gluing these simplices ‘nicely’ together along their edges and faces. There are many types of SCs, but here we are using what is known Vietoris-Rips (Rips) SCs as it is easy to construct and compute in comparison with other types of SCs. Traditional construction of Rips SCs are based on selecting a single distance threshold and calculating corresponding topological invariants such as betti numbers (β_n for $n = 0,1,2$), Euler characteristics, cliques and other topological invariants.

The popular mathematical theory used to characterise topological features is known as homology theory. More precisely, the rank of the n -th homology group equals to what is known as betti numbers β_n , where β_0 is equal to the number of connected components (CCs), β_1 is the number of holes and β_2 is the number of cavities in the constructed Rips SC. Instead of computing aforementioned topological invariants at a single distance threshold, TDA depends on calculating the persistency of these invariants across an increasing series of distance thresholds using what is known as persistent homology ^{(9), (10)}.

The first step in building a SC is to consider landmark points (i.e. zero-dimensional simplices) in order to be able to build on them higher dimensional simplices such as edges, triangles and tetrahedrons. For this task, the approach suggested in ⁽¹¹⁾ is followed which is the use of uniform Local Binary Patterns as a tool to systematically choose landmark points from images of interest to build topological objects.

Local Binary Patterns (LBP)

Ojala *et al.* in ⁽¹²⁾ first introduced LBP as an image texture descriptor. In this papaer, the original idea proposed in ⁽¹²⁾ is followed. Given any image, LBP replaces each pixel of the image with an 8-bit binary code, which encapsulates texture and local structure, determined by its 8 neighbouring pixels in a 3×3 window surrounding it in clockwise order, see **Figure 1**. The process works as follow: starting from the top-left corner of the window; subtract central pixel from its 8 neighbouring pixels, assign 0 if the result is negative, and 1 otherwise. Mathematically this process can be written as follow:

$$LBP(x_c, y_c) = \sum_{i=1}^7 \alpha(P_i - P_c)2^i \tag{1}$$

Where P_i is the neighboring grey value pixels, P_c is the center grey value pixel, and the function $\alpha(x)$ is as follow:

$$\alpha(x) = \begin{cases} 1 & \text{if } x \geq 0 \\ 0 & \text{if } x < 0 \end{cases} \tag{2}$$

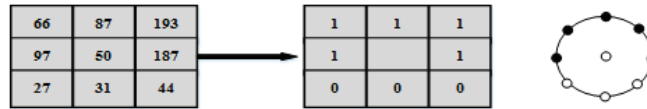


Figure 1: An example of Local Binary Operator.

Uniform LBP (ULBP) refers to 8-bit circular bytes that have no more than 2 circular transitions. For the sake of clarity, examples of ULBPs are 11110000 (2 transitions), 11111111 (0-transitions) and examples of non-uniform LBP are 10101010 (8-transitions), 11001110 (4 transitions). This means that ULBP of any monochrome image consists of 58 unique uniform geometries, see **Figure 2**. It has been shown that ULBP codes constitute 90% of LBP codes in natural images⁽¹³⁾. There are seven groups (of 8 binary codes) of ULBP according to the number of 0's and 1's in their binary codes, excluding the cases 00000000 and 11111111. Each of these groups is related to certain types of image textures. The ULBP codes have t consecutive 1's as geometry- t . Our experimental investigation contains the set of pixels in all geometries as potential landmark candidates to build SC.

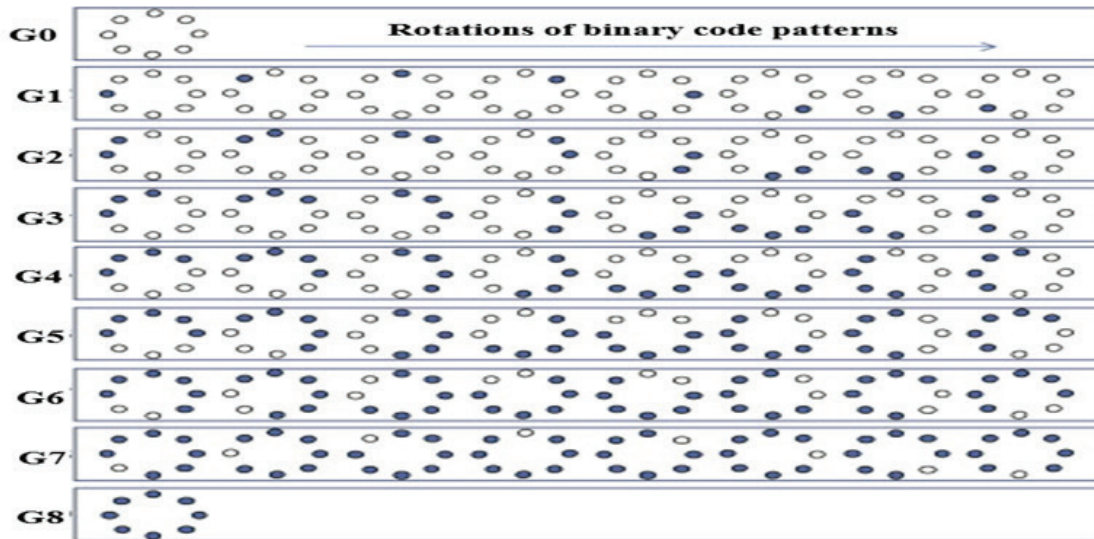


Figure 2: The 58 different uniform patterns in (8, 1).

Regarding uniform LBP patterns classifications based on the number of ones included in the pattern in the natural images database which described in⁽¹⁴⁾, the patterns in G0, G8, (G2 and G4), (G3 and G5), and G6 describe the flat area, spot area, edges, corners, and line ends in the image, respectively.

Construction of Rips Simplicial Complexes

For each class of geometry- t in ULBP, its

corresponding positions are extracted in the forged and original images of the given data. As a result, we end up with a set of image pixel positions of the 8 sets of t -ones ULBP codes. First, the known Euclidean distance is calculated between all pairs of points in the set, and then an increasing 8 sequence of T -dependent Rips complexes is constructed, one for each rotation of the geometry- t codes. For $T = 0$, only 0-dimensional

simplices are obtained, i.e. the points. Then T is gradually increased and computed β_0 at each T .

Robert Ghrist in ⁽¹⁰⁾ illustrated that there is no optimal method to select the best threshold that best captures the topology of data sets. A fixed number of distance thresholds are used, as follows:

$$T_1 = 0, T_2 = 3, T_3 = 5, T_4 = 7, T_5 = 10, T_6 = 12, T_7 = 15, T_8 = 17, T_9 = 20$$

This approach is motivated by the work of A. Asaad and S. Jassim in ⁽¹¹⁾, as they used the TDA approach to assess the quality of degraded images. In particular, they focused on discriminating face images degraded by shadows and blurring. The topological invariant which is used across this paper is the zero homology groups, which correspond to the number of CCs, as shown in **Figure 3**.

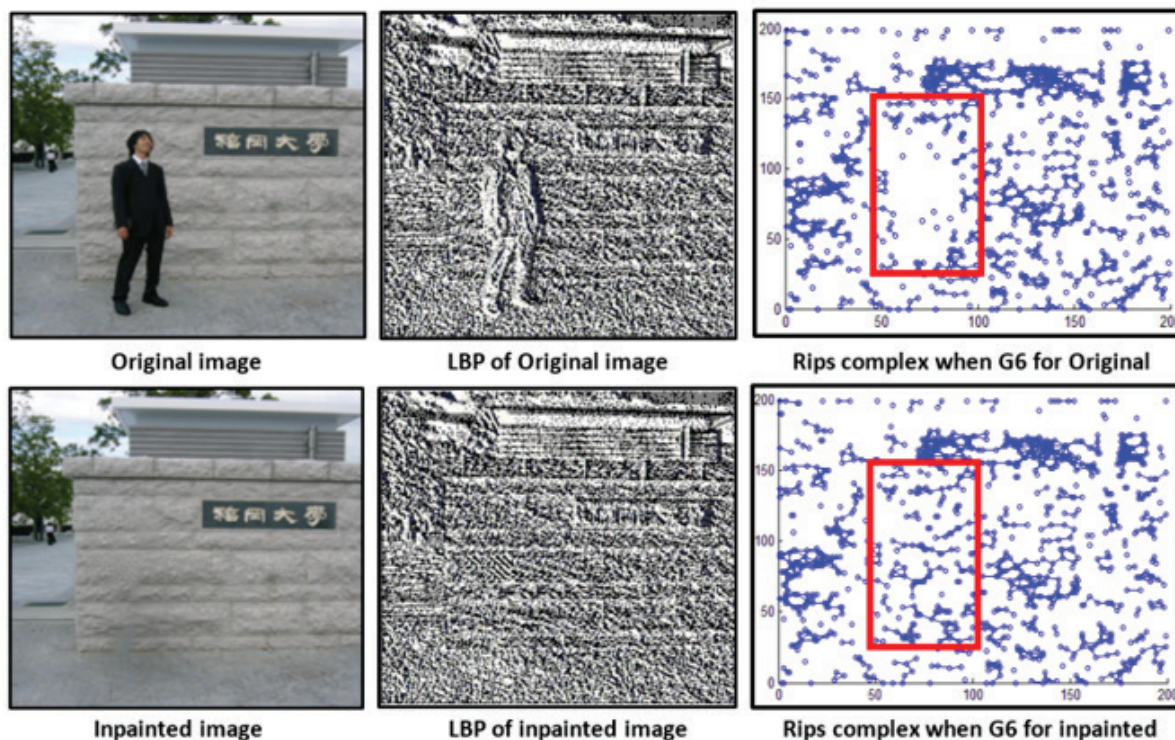


Figure 3: LBP and simplicial complexes of the original and forged image at threshold T=10.

More specifically, the Rips complex graph for forged image and the original image are identical, except the forged region which we highlighted by red box in **Figure 3**. The TDA approach is used to detect forged images by counting the number of CCs in the images, where the CCs is computed in 8 rotations in each one of these 7 geometries at different thresholdings.

Forgery detection-based TDA approach

A new forensic technique is proposed to detect the forged images using the TDA approach. The steps of the proposed technique are as follows:

- 1) Image pre-processing: Before the features extraction process, converting these RGB images into a grayscale images, then transforming them into the LBP domain.
- 2) Feature extraction: Applying the TDA approach to the LBP image domain, the number of CCs will be counted in each geometry (i.e. G1, G2,..., G7) at different thresholds (i.e. T=0, T=3, T=5, T=7, ...) until the number of the CCs be 1 in each rotation.
- 3) Classification: The purpose of a classifier is to discriminate the given images and classify them into two

categories which are original and forged images based on the number of CCs in each geometry at different thresholds. The kNN classifier method is used to classify the images into two groups which are original and forged groups (i.e. decision stage) ^{(15), (16)}.

Testing Experiments

The forgery proposed method is applied to detect forged images from the yokoya natural database in ⁽¹⁷⁾, which consists of 100 original and 100 forged (inpainted) images of size 200200, as see in **Figure 4**.



Figure 4: Example of six out of 100 training natural images.

To detect the inpainted images, the TDA approach is used by selecting landmarks from the whole image to build SCs and then computed their corresponding homological features (ie. the number of CCs). The number of CCs is computed from different increasing distance thresholds and the pattern of change in the components while we increase the threshold is stored. We stop when the number of CCs becomes one for both classes (original and inpainted images). Finally, we train kNN classifier when k=1 (i.e. Nearest Neighbour) on those 200 images with 3 different classification protocol as follow:

- Protocol One: 30% of the data used for Training

- Protocol Two: 50 % of the data used for Training
- Protocol Three: 70% of the data used for training.

Each protocol is repeated 100 times, across seven ULBP groups and 10 different increasing distance thresholds. Experimental results showed the number of CC is sensitive to the degradation present in the inpainted images. Furthermore, among the 7 geometries we used as landmarks to build the topology G1, G5 and G7 geometries more sensitively detect the changes in the edges and corners in the inpainted images ⁽¹⁸⁾, as see in the **Tables 1**.

Table 1: kNN classifier on CCs features from natural images.

Training / 30, kNN classifier/Accuracy								Training / 50, kNN classifier/Accuracy								Training / 70, kNN classifier/Accuracy							
T	G1	G2	G3	G4	G5	G6	G7	T	G1	G2	G3	G4	G5	G6	G7	T	G1	G2	G3	G4	G5	G6	G7
T=0	56.35	53.66	54.22	54.13	55.47	53.04	52.97	T=0	59.81	54.71	55.61	54.91	57.36	53.84	55.36	T=0	62.43	57.06	57.36	56.76	58.66	54.95	58.03
T=3	58.85	54.16	55.67	53.12	55.85	53.65	56.14	T=3	61.55	57.57	58.92	54.48	57.11	55.38	59.25	T=3	64.56	61.01	59.48	55.46	58.5	57.95	62.28
T=5	59.52	56.78	57.27	58.22	63.57	57.93	64.07	T=5	62.83	60.05	59.85	60.48	66.53	61.36	66.17	T=5	67.46	63.83	62.46	64.08	71.01	61.23	68.55
T=7	65.95	58.25	59.8	60.29	64.82	57.07	67.21	T=7	68.18	61.23	62.77	63.19	67.59	60.26	70.14	T=7	71.66	65.36	66.63	65.15	70.77	63.45	73.15
T=9	83.62	68.23	67.28	66.99	68.37	66.07	84.86	T=9	84.84	71.63	70.81	69.93	78.67	67.86	86.95	T=9	87.63	74.41	74.11	73.88	80.66	69.38	88.61
T=10	91.35	74.88	72.7	67.52	80.62	69.49	92.87	T=10	89.74	77.01	79.28	76.17	83.26	71.43	93.94	T=10	90.87	78.61	78.76	72.16	86.38	71.76	94.81
T=12	78.57	64.58	65.68	65.11	72.69	63.76	78.92	T=12	79.36	68.27	68.44	66.41	72.97	65.09	80.36	T=12	81.18	70.31	70.17	69.67	75.88	66.15	81.83
T=15	68.91	58.77	62.51	60.45	68.82	61.77	70.25	T=15	71.47	61.44	64.96	62.61	70.71	63.76	72.35	T=15	73.86	68.37	68.36	64.33	72.14	64.06	75.36
T=17	58.12	56.54	53.22	54.57	58.51	55.57	63.85	T=17	62.15	59.37	54.95	58.79	59.81	56.18	66.53	T=17	67.96	56.8	56.31	59.53	60.98	56.26	68.83
T=20	53.67	50.27	52.03	51.97	55.83	50.78	52.97	T=20	55.47	52.19	52.58	51.68	58.93	52.08	54.97	T=20	57.21	54.32	53.33	52.38	60.16	52.91	56.95

Examining the whole distribution of accuracies from T=0 to T=20, the accuracy is starting in a low rate around 52% then gradually increasing until reach the peak at T=10 and then gradually decreasing. The highest obtained accuracy is 90% for detecting the

inpainted images at T=10. Also, the number of images in the training does not affect the accuracy of the image classification, that means the classification features are strong.

The values of accuracy for classifying the natural images into original and inpainted images are not absolutely correct. There are two kinds of error which are False Positive (FP) and False Negative (FN). The FP represents the original images that classify as forged

images, while FN represents the forged images that classify as original images⁽¹⁹⁾. **Tables 2** show the average of FP and FN values for each geometry at different thresholds in above three protocols, respectively.

Table 2: False Positive and False Negative values from natural images.

Training / 30, kNN classifier/False Positive								Training / 50, kNN classifier/False Positive								Training / 70, kNN classifier/False Positive							
T	G1	G2	G3	G4	G5	G6	G7	T	G1	G2	G3	G4	G5	G6	G7	T	G1	G2	G3	G4	G5	G6	G7
T=0	27.51	28.21	31.03	24.89	26.06	25.98	30.11	T=0	17.95	19.54	21.32	16.88	18.13	17.62	20.06	T=0	17.95	19.54	21.32	16.88	18.13	17.62	20.06
T=3	27.91	28.5	29.11	26.58	27.94	30.46	26.02	T=3	19.02	19.05	18.42	17.92	18.95	20.12	16.21	T=3	19.02	19.05	18.42	17.92	18.95	20.12	16.21
T=5	28.66	28.11	29.67	26.84	25.32	28.55	25.75	T=5	19.17	18.39	19.98	18.88	16.67	19.14	17.45	T=5	19.17	18.39	19.98	18.88	16.67	19.14	17.45
T=7	24.62	30.13	26.82	24.57	23.49	30.06	25.39	T=7	16.41	19.81	17.02	15.79	15.27	19.16	15.71	T=7	16.41	19.81	17.02	15.79	15.27	19.16	15.71
T=9	11.08	24.63	23.44	20.81	20.73	24.15	8.58	T=9	7.86	16.17	15.28	13.93	9.56	16.09	5.23	T=9	7.86	16.17	15.28	13.93	9.56	16.09	5.23
T=10	6.43	17.91	16.58	21.88	12.41	21.98	4.09	T=10	4.42	12.43	9.78	12.09	7.73	13.49	2.54	T=10	4.42	12.43	9.78	12.09	7.73	13.49	2.54
T=12	13.07	28.87	24.23	19.94	17.24	25.96	12.21	T=12	8.71	18.82	15.53	13.36	12.48	17.87	8.27	T=12	8.71	18.82	15.53	13.36	12.48	17.87	8.27
T=15	26.14	29.21	27.68	29.28	15.18	17.59	28.99	T=15	17.18	19.43	18.32	19.66	9.93	11.49	19.32	T=15	17.18	19.43	18.32	19.66	9.93	11.49	19.32
T=17	23.51	25.71	28.38	26.71	22.86	34.06	16.12	T=17	14.56	16.85	18.98	17.68	15.72	22.75	10.73	T=17	14.56	16.85	18.98	17.68	15.72	22.75	10.73
T=20	24.71	27.29	27.16	29.59	28.01	28.77	19.46	T=20	15.55	17.35	18.61	16.91	18.36	18.04	12.57	T=20	15.55	17.35	18.61	16.91	18.36	18.04	12.57

Training / 30, kNN classifier/False Negative								Training / 50, kNN classifier/False Negative								Training / 70, kNN classifier/False Negative							
T	G1	G2	G3	G4	G5	G6	G7	T	G1	G2	G3	G4	G5	G6	G7	T	G1	G2	G3	G4	G5	G6	G7
T=0	33.62	36.66	33.06	39.32	36.27	39.76	35.84	T=0	22.24	25.75	23.07	28.21	24.51	28.54	24.58	T=0	12.66	14.76	13.67	16.33	14.59	18.07	14.31
T=3	29.78	35.67	32.95	39.04	33.86	34.42	35.38	T=3	19.43	23.38	23.66	27.63	23.94	24.52	24.54	T=3	10.29	13.23	14.29	16.94	13.83	14.08	14.54
T=5	28.76	32.56	30.14	31.65	25.78	30.34	24.54	T=5	18.21	21.56	20.17	20.64	16.86	19.58	16.45	T=5	9.44	11.88	11.23	11.19	8.81	12.85	8.95
T=7	23.07	28.31	29.45	31.02	25.76	30.04	20.52	T=7	15.42	18.96	20.21	21.02	17.14	20.64	14.16	T=7	8.32	10.06	10.83	11.53	9.33	11.85	7.84
T=9	11.84	19.84	22.36	25.41	23.54	23.34	12.61	T=9	7.31	12.27	13.91	16.14	11.83	16.05	7.82	T=9	3.44	6.62	7.27	8.72	6.25	9.56	4.22
T=10	6.16	17.25	21.63	23.38	14.72	20.73	5.89	T=10	5.88	10.56	10.94	11.74	8.01	15.08	3.52	T=10	2.89	5.48	2.59	6.74	4.67	8.96	1.85
T=12	16.92	20.71	23.81	28.91	20.99	24.77	17.31	T=12	11.93	12.93	16.07	20.23	14.55	17.11	11.44	T=12	6.79	7.71	9.54	11.43	7.75	9.95	6.04
T=15	17.38	28.52	24.82	26.08	28.47	35.93	12.66	T=15	11.42	19.23	16.72	17.79	19.37	25.51	8.33	T=15	6.29	9.33	9.33	10.37	10.53	14.96	4.43
T=17	35.13	35.14	37.17	36.91	35.23	28.24	34.48	T=17	23.29	23.78	26.07	23.53	24.47	21.07	22.74	T=17	12.23	12.79	15.53	14.31	14.23	12.69	12.15
T=20	40.15	42.32	39.99	37.65	33.82	40.13	46.37	T=20	28.98	30.46	28.81	31.41	22.71	29.88	32.46	T=20	17.43	15.94	16.91	19.29	13.37	17.91	19.09

Tables 2 showed the average values of FP and FN in G1, G5, and G7 at threshold T=10 are less than in other geometries and in other thresholds. This clearly shows that TDA can be used as an effective technique for inpainting detection.

Summary and Conclusion

A novel forgery detection technique has been proposed to recognise tampered inpainting images (i.e. by the EBI method). TDA has been used to detect the forged images (i.e. to detect which of these images has had an object removed from it). The number of CCs has been used as a component in the feature vector in the classifier methods. The kNN classifier has been used to classify the images into original and forged images. The proposed method has been applied to natural database images. The experimental results showed that the proposed method performs well in detecting inpainted images with promising results. Also, the FP and FN error are calculated for all geometries at different thresholds for natural database images. In the future, we will extend our investigation to detect the suspicious regions in the forged image by applying TDA approach.

Ethical Clearance: Taken from applied computing school, buckingham university committee.

Source of Funding: Self.

Conflict of Interest: It is nil.

References

1. Birajdar GK, Mankar VH. Digital image forgery detection using passive techniques: A survey. Digit Investig. 2013;10:226–45.
2. Qiong Wu, Shao-Jie Sun, Wei Zhu, Guo-Hui Li, Dan Tu. Detection of digital doctoring in exemplar-based inpainted images. In: 2008 International Conference on Machine Learning and Cybernetics. IEEE; 2008. p. 1222–6.
3. Chang IC, Yu JC, Chang CC. A forgery detection algorithm for exemplar-based inpainting images using multi-region relation. Image Vis Comput. 2013;31(1):57–71.
4. Bacchuwar KS, Aakashdeep, Ramakrishnan KR. A jump patch-block match algorithm for multiple forgery detection. In: 2013 International Mutli-Conference on Automation, Computing, Communication, Control and Compressed Sensing (iMac4s). IEEE; 2013. p. 723–8.
5. Liang Z, Yang G, Ding X, Li L. An efficient forgery detection algorithm for object removal by exemplar-based image inpainting. J Vis Commun Image Represent. 2015 Jul;30(C):75–85.

6. Yang G, Tools Appl M, Zhang D, Liang Z, Li Q, Li L, et al. A robust forgery detection algorithm for object removal by exemplar-based image inpainting. 2017;
7. Carlsson G. TOPOLOGY AND DATA. *Bull New Ser Am Math Soc.* 2009;46(209):255–308.
8. Lum PY, Singh G, Lehman A, Ishkanov T, Vejdemo-Johansson M, Alagappan M, et al. Extracting insights from the shape of complex data using topology. *Sci Rep.* 2013 Dec;3(1):1236.
9. Edelsbrunner H. PERSISTENT HOMOLOGY: THEORY AND PRACTICE. Ernest Orlando Lawrence Berkeley Natl Lab Berkeley, CA. 2012;LBNL-6037E.
10. Ghrist R. Barcodes: The persistent topology of data. In: *Bulletin of the American Mathematical Society.* 2008. p. 61–75.
11. Asaad AT, Rashid RD, Jassim SA. Topological image texture analysis for quality assessment. In: Agaian SS, Jassim SA, editors. *International Society for Optics and Photonics*; 2017. p. 102210I.
12. Ojala T, Pietikäinen M, Harwood D. A comparative study of texture measures with classification based on featured distributions. *Pattern Recognit.* 1996 Jan;29(1):51-9.
13. Ahonen T, Hadid A, Pietikainen M. Face Description with Local Binary Patterns: Application to Face Recognition. *IEEE Trans Pattern Anal Mach Intell.* 2006 Dec;28(12):2037–41.
14. Ojala T, Pietika M, Ma T. Multiresolution Gray-Scale and Rotation Invariant Texture Classification with Local Binary Patterns. 2002.
15. Cover T, Hart P. Nearest neighbor pattern classification. *IEEE Trans Inf Theory.* 1967 Jan;13(1):21–7.
16. Chen CH, Wang PSP. *Handbook of Pattern Recognition and Computer Vision.* WORLD SCIENTIFIC; 2005.
17. yokoya. 100 images used in the restoration experiments. restoration images Data set.
18. Ojala T, Pietikainen M, Maenpaa T. Multiresolution gray-scale and rotation invariant texture classification with local binary patterns. *IEEE Trans Pattern Anal Mach Intell.* 2002 Jul;24(7):971–87.
19. Warwick-Evans VC, Atkinson PW, Robinson LA, Green JA. Predictive Modelling to Identify Near-Shore, Fine-Scale Seabird Distributions during the Breeding Season. Hemelrijk CK, editor. *PLoS One.* 2016 Mar;11(3):e0150592.